

Enhancing red-shifted white-light continuum generation in optical fibers for applications in nonlinear Raman microscopy

Georgi I. Petrov, and Vladislav V. Yakovlev

Department of Physics, University of Wisconsin – Milwaukee, P. O. Box 413,
Milwaukee, WI 53201, USA
yakovlev@uwm.edu

Abstract: We report an efficient red-shifted continuum generation of picosecond pulses in conventional optical fibers. By using a novel high-repetition rate, high-energy oscillator operating at the fundamental wavelength of 1064 nm, we achieved more than 60% of the output energy in the spectral range from 1150 to 1300 nm, perfectly suitable for broadband coherent anti-Stokes Raman spectroscopy.

©2005 Optical Society of America

OCIS codes: 170.5660 Raman spectroscopy, 180.0180 Microscopy, 190.0190 Nonlinear optics, 190.5890 Scattering, stimulated, 320.0320 Ultrafast optics

References and Links

1. T. Hirschfeld, "Raman microprobe: vibrational spectroscopy in the femtogram range," *J. Opt. Soc. Am.* **63**, 476 (1973).
2. J. R. Lakowicz, *Principles of fluorescent spectroscopy*, Plenum Press, New York, 1983.
3. B. S. Hudson, "New laser techniques for biophysical studies," *Ann. Rev. of Biophys. Bioengin.* **6**, 135-150 (1977).
4. T. Wilson, *Confocal microscopy*, Academic Press, London, 1990.
5. M. D. Duncan, J. Reintjes, and T. J. Manuccia, "Scanning coherent anti-Stokes Raman microscope," *Opt. Lett.* **7**, 350-352 (1982).
6. A. Zumbusch, G. R. Holton, and X. S. Xie, "Three-dimensional vibrational imaging by coherent anti-Stokes Raman scattering," *Phys. Rev. Lett.* **82**, 4142-4145 (1999).
7. E. O. Potma, W. P. de Boeij, P. J. M. van Haastert, and D. A. Wiersma, "Real-time visualization of intracellular hydrodynamics in single living cells," *Proc. Natl. Acad. Sci.* **98**, 1577-1582 (2001).
8. M. Hashimoto, and T. Araki, "Molecular vibration imaging in the fingerprint region by use of coherent anti-Stokes Raman scattering microscopy with a collinear configuration," *Opt. Lett.* **25**, 1768-1770 (2000).
9. V. V. Yakovlev, "Real-time nonlinear Raman microscopy," in *Biomedical Diagnostic, Guidance, and Surgical-Assist Systems III*, T. Vo-Dinh, V. S. Grundfest, D. A. Benaron, eds., *Proc. SPIE* **4254**, 97-105 (2000).
10. G. W. H. Wurpel, J. M. Schins, and M. Müller, "Chemical specificity in three-dimensional imaging with multiplex coherent anti-Stokes Raman scattering microscopy," *Opt. Lett.* **27**, 1093-1095 (2002).
11. N. Dudovich, D. Oron, and Y. Silberberg, "Single-pulse coherently controlled nonlinear Raman spectroscopy and microscopy," *Nature* **418**, 512-514 (2002).
12. V. V. Yakovlev, "Advanced instrumentation for non-linear Raman microscopy," *J. Raman Spectrosc.* **34**, 957-964 (2003).
13. V. V. Yakovlev, "Broadband cost-effective nonlinear Raman microscopy," in *Multiphoton Microscopy in Biomedical Sciences IV*, A. Periasamy, P. T. C. So, eds., *Proc. SPIE* **5323**, 214-222 (2004)
14. V. Tuchin, *Tissue optics*, SPIE Press, Bellingham, WA, USA, 2000.
15. K. König, T. W. Becker, P. Fischer, I. Riemann, and K. J. Halhuber, "Pulse-length dependence of cellular response to intense near-infrared laser pulses in multiphoton microscopes," *Opt. Lett.* **24**, 113-115 (1999).
16. J. M. Squirrell, D. L. Wokosin, J. G. White, and B. D. Bavister, "Long-term two-photon fluorescence imaging of mammalian embryos without compromising viability," *Nat. Biotech.* **17**, 763-767 (1999).
17. B. N. Toleutaev, T. Tahara, and H. Hamaguchi, "Broad-band (1000 cm⁻¹) multiplex CARS spectroscopy – application to polarization-sensitive and time-resolved measurements," *Appl. Phys.* **B59**, 369-375 (1994).
18. V. H. Astinov, and G. M. Georgiev, "Ultrabroadband single-pulse CARS of liquids using a spatially dispersive Stokes beam," *Appl. Phys.* **B63**, 62-68 (1996).
19. G. I. Petrov, V. V. Yakovlev, and N. I. Minkovski, "Near infrared continuum generation of femtosecond and picosecond pulses in doped optical fibers," *Appl. Phys.* **B77**, 219-226 (2003).

20. G. I. Petrov, V. V. Yakovlev, and N. I. Minkovski, "Broadband nonlinear optical conversion of a high-energy diode-pumped picosecond laser," *Opt. Commun.* **229**, 441-445 (2004).
21. K. A. Stankov, "A mirror with an intensity-dependent reflection coefficient," *Appl. Phys.* **B 45**, 191-195 (1988).
22. A. Agnesi, C. Pennacchio, G. C. Reali, and V. Kubecek, "High-power diode-pumped picosecond Nd³⁺:YVO₄ laser," *Opt. Lett.* **22**, 1645-1647 (1997).
23. R. R. Alfano, Ed. *The supercontinuum laser source* (Springer-Verlag, New York, 1989).
24. E. M. Dianov, "Advances in Raman fibers," *J. Lightwave Technol.* **20**, 1457-1462 (2002).
25. D. I. Chang, S. V. Chernikov, M. J. Guy, J. R. Taylor, and H. J. Kong, "Efficient cascaded Raman generation and signal amplification at 1.3 μm in GeO₂-doped single-mode fibre," *Opt. Commun.* **142**, 289-293 (1997).
26. H. S. Seo, and K. Oh, "Optimization of silica fiber Raman amplifier using the Raman frequency modeling for an arbitrary GeO₂ concentration in the core," *Opt. Commun.* **181**, 145-151 (2000).
27. J. X. Cheng, Y. K. Jia, G. F. Zheng, and X. S. Xie, "Laser-scanning coherent anti-stokes Raman scattering microscopy and applications to cell biology," *Biophys. J.* **83**, 502-509 (2002).
28. A. Volkmer, L. D. Book, and X. S. Xie, "Time-resolved coherent anti-Stokes Raman scattering microscopy: Imaging based on Raman free induction decay," *Appl. Phys. Lett.* **80**, 1505-1507 (2002).
29. G. I. Petrov, S. Saltiel, R. D. Heathcote, and V. V. Yakovlev, "Nonlinear microscopy of cellular structures," *Las. Phys. Lett.* **1**, 10-15 (2004).
30. G. I. Petrov, V. Shcheslavskiy, L. Sona, and V. V. Yakovlev, "CARS-microscopy analysis of collagen transformation," in *Multiphoton Microscopy in Biomedical Sciences V*, A. Periasamy, and P. T. C. So, eds., *Proc. SPIE* **5700** (2005) In press.

1. Introduction

Non-invasive microscopic imaging of biological systems remains a key problem in understanding the relationship between structure and function on the cellular and molecular levels. Vibrational spectroscopy is typically considered as one of the most informative, truly non-invasive optical techniques capable of providing valuable information on the structure and function of molecules. Raman spectroscopy and microscopy are particular important, since they can provide sub-micron spatial resolution. Since the first introduction of Raman microscope in 1973 [1], optical and laser technology has made a tremendous step forward. The availability of inexpensive, energy efficient, stable and reliable laser sources together with improved technology for spectral filtering and multichannel detection greatly increased our ability to study inorganic and organic materials in picoliter volumes. Raman confocal systems, which are now commercially available, permit rejections out of focus signal, making possible high contrast high resolution non-invasive imaging. However, Raman microscopy is still considered an emerging technique for biological imaging. Despite of the obvious advantages of being very informative and almost nondestructive method of studying biological molecules, classical Raman spectroscopy (spectroscopy, using spontaneous Raman scattering) suffers from a series of limitations, such as a fluorescent background and a low signal level. Thus, fluorescent spectroscopy is often used, when real-time measurements are required [2]. On the other hand, nonlinear Raman spectroscopy, and, in particular, spectroscopy of coherent anti-Stokes Raman scattering (CARS), can resolve most of the problems associated with conventional Raman spectroscopy [3]. First, being a nonlinear optical method of spectroscopy, CARS spectroscopy relies on interaction of high intensity laser pulses. Since intensity of these pulses is the highest in the focal point of a microscope, CARS spectroscopy offers excellent discrimination against out of focus points. A nonlinear optical Raman microscope will be an ideal confocal microscope without using an additional aperture [4], thus greatly increasing the signal collection efficiency. Second, nonlinear Raman spectroscopy provides a way to increase a signal's level by increasing the intensity of incoming pump pulses. For ultrashort (picosecond (i.e. 10^{-12} s) pulses, a signal's level can be as much as several orders of magnitude higher than that for conventional Raman spectroscopy for a given average power of the incident laser beam [3]. Third, the detected signal is blue-shifted with respect to the excitation wavelengths, thus there is no problem of separating the signal from a fluorescent background. Fourth, short pulse lasers, used for CARS

spectroscopy, naturally designed to study ultrafast processes on the molecular scale, thus giving a unique opportunity to study molecular transformations (such as protein folding, DNA transformations, etc.) in a real-time (i.e. on the time scale of molecular processes). Finally, red and IR photons (which can be used in a nonlinear optical Raman microscope, because of its superior efficiency even for non-resonant transitions) are much better at penetrating biological tissues, because fewer biological molecules absorb them and because light scattering is less at longer wavelengths. All these features of a nonlinear optical spectroscopy of vibrational molecular modes turn out to be extremely useful for overcoming major problems in a Raman microscopy of living specimens. The development and exploration of a nonlinear Raman microscope represents a significant step forward in the field of optical microscopy and a substantial new approach in real-time diagnostics.

Nonlinear Raman microscopy was first introduced for biological imaging in 1982 [5], however, the complexity of experimental set-up based on dye laser technology limited the applicability of this technique. The new era of CARS microscope started several years ago, when solid-state ultrafast laser sources became widely available. Several groups [6-12] have explored the variety of instrumental approaches to nonlinear Raman imaging. Despite of significant advances in terms of stability and overall reliability of newly developed generation of nonlinear Raman microscopes, all of them suffer from a significant complexity, resulting in a total price of a laser system alone to be of the order of several hundred thousand dollars. This limits the wide spread of nonlinear Raman microscopy and further development of it as a spectroscopic tool for biological, and in a future perspective, biomedical imaging.

Recently, we introduced a novel concept of a simple, compact and significantly less expensive approach to CARS microscopy [9, 12-13], which offers broadband capability and high spectra resolution.

2. System design considerations

CARS spectroscopy requires at least two beams of different colors: ω_1 and ω_2 . If the difference between these frequencies equals the frequency of molecular vibration $\Omega = \omega_1 - \omega_2$, then due to nonlinear optical interactions of laser light with molecules several different waves are produced as a result of a coherent scattering of incident photons ω_1 and ω_2 on molecular vibrations. Assuming that ω_1 is greater than ω_2 , the most important is $\omega_{\text{CARS}} = \omega_1 + \Omega$, which is blue-shifted with respect to the incident frequencies and any fluorescent background (which is red-shifted with respect to both ω_1 and ω_2) will not suppress the useful signal. CARS microscopy, being a third-order nonlinear-optical process, benefits from using ultrashort laser pulses. However, when the pulse duration becomes so short that its bandwidth is broader than the bandwidth of typical Raman lines ($\Delta\nu=3-5 \text{ cm}^{-1}$), the efficiency of this nonlinear process goes down with further decrease of the pulse duration [9, 12]. From these considerations we conclude that a pair of synchronized picosecond pulses is required for successful CARS microscopy.

There are several advantages of using longer wavelength for CARS microscopy. First, the penetration depth dramatically increases for the spectral range from 1- μm to 1.3- μm , due to the reduced scattering [14]. Secondly, the damage threshold for a typical tissue increases manifold by a relatively modest shift excitation wavelength to IR (in our results we compared excitation of 800 nm and 1250 nm light, similar results have been earlier reported for 800 nm and 1000 nm excitation [9, 12, 15-16]). If the excitation wavelength is longer than 1- μm , it is practically invisible for Si-based detectors, whose sensitivity drops dramatically above 1000 nm. Since the generated CARS signal is blue shifted with respect to pump wavelengths, it will be easier to filter this signal from the residual pump radiation. For a biologically important spectral region from 1400 to 1700 cm^{-1} CARS signal will be just near the maximum of the sensitivity curve for a typical Si detector. Finally, the move from Ti:sapphire laser based technology to a more established Nd^{3+} -doped laser materials represents the major shift in

terms of the simplification of laser technology for CARS imaging. Picosecond and even femtosecond lasers utilizing Nd^{3+} -doped gain media are readily available and can be diode-pumped using relatively inexpensive laser diodes. This part of the paper describes a simple and inexpensive (we estimate the total cost of all opto-mechanical components including microscope set-up and microscope objectives to be less than \$50,000), but reliable way of producing picosecond pulses for CARS imaging.

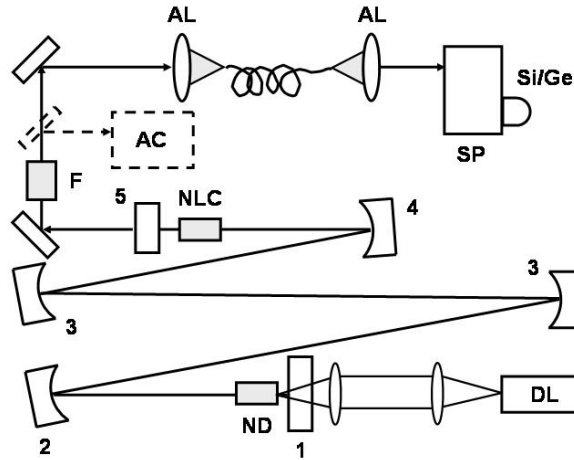


Fig. 1. Laser set up. DL – diode laser, ND – $\text{Nd}^{3+}:\text{YVO}_4$ crystal, Ge/Si – mixed Ge/Si photodetector, SP – spectrometer, F – Faraday isolator, NLC – nonlinear optical crystal, AC – autocorrelator, AL – aspheric lens, 1 – flat mirror (HR @ 1064 nm, HT @ 808 nm), 2 – concave mirror (R = 0.5 m; HR @ 1064 nm), 3 – concave mirror (R = 2.0 m; HR @ 1064 nm), 4 – concave mirror (R = 0.3 m; HR @ 1064 nm), 5 – flat output coupler (HR @ 532 nm, T = 78% @ 1064 nm). For simplicity a laser resonator with a single pass through the telescopic optics (3) is shown.

The key idea of our laser design is based on utilizing broadband CARS microscopy [17-18]. We will use a narrow band pulse at one pump wavelength (ω_1), and a broadband pulse at another pump wavelength (ω_2). Since for most of applications it is required to take the whole Raman spectrum for molecular identification, it would be wise to use a broadband CCD detector coupled to a spectrometer to take the whole CARS spectrum all in the same time. As a narrowband pulse, we will use the fundamental output of the Nd^{3+} -doped laser, and as a broadband pulse we can use a spectrally selected broadband portion of a continuum generated from a part of the fundamental output. This way, two pump pulses are temporarily synchronized to each other and both have picosecond pulse duration.

3. Experimental set up

Recently we have constructed a diode-pumped picosecond $\text{Nd}:\text{YVO}_4$ laser that can generate a synchronized broad-band continuum in a specially designed optical fiber [19-20].

We use a 12-W fiber-coupled diode laser ($\lambda = 808$ nm (LIMO, Ltd.)) to pump a 5 mm long $\text{Nd}:\text{YVO}_4$ crystal to generate 1064 nm radiation. To initiate mode-locking we use a “nonlinear-optical-mirror” self-starting mechanism [21-22]. Our experimental set-up is sketched in Fig. 1. The 4-mm-long LBO crystal is used as a nonlinear optical medium. The second harmonic generated in this crystal on the first pass is then reflected from the back mirror (HR @ 532nm, R=80% @ 1064 nm). On the way back the second-harmonic wave can be back converted to a fundamental frequency (under certain conditions) providing positive feedback to initiate mode locking. We use an intracavity telescope to extend the length of the

laser cavity. It results in lowering the repetition rate of the laser pulses and increased energy per pulse promoting nonlinear interactions, and providing better overall stability. Pulses as short as 4-ps are routinely generated [20]. Since the pulse duration depends only on the nonlinear crystal length, no pulse-length fluctuations are allowed in the system leading to a very stable train of pulses at a repetition rate of 15-100 MHz with a total power of up to 3 W.

It is rather challenging to generate broad-band continuum using picosecond pulses. The mechanism of self-phase-modulation is generally considered to be the dominant mechanism for spectral broadening of ultrashort pulses. The time dependent shift of instantaneous frequency can be expressed using the following formula [23]:

$$\Delta\omega(t) = -\omega_0 \frac{n_2 \cdot L}{c} \frac{dI(t)}{dt}, \quad (1)$$

where $I(t)$ is temporal intensity profile, L is the propagation length, ω_0 is a carrier frequency, and n_2 is the nonlinear refractive index of the medium. It is clear that this mechanism benefits from the decrease of the pulse duration. When picosecond pulses are used, longer propagation length, L , is required and dispersion becomes important. Most recent progress in photonic crystal fiber engineering allows partial solution of this problem by accurate dispersion management. However, the efficient energy conversion has not been demonstrated yet.

Recently we suggested that stimulated Raman scattering may play an important role in enhancing the efficiency of red-shifted white-light continuum [19]. By doping silica fiber with germania, the threshold for stimulated Raman scattering decreases manifold [19]. The Raman spectrum of GeO₂-SiO₂ fiber [24] is somehow similar to one of a traditional SiO₂ fiber – it also has a broad Raman band centered ~430 cm⁻¹, however the intensity of this band is much stronger, and its strength almost linearly depends on the GeO₂ doping concentration [25]. It has been demonstrated that Raman gain increases linearly with the GeO₂ doping and can be 9.2 times higher than that of a pure silica fiber [26]. This high Raman cross-section leads to stimulated Raman scattering, which shifts the incident wavelength further into infrared. Although stimulated Raman scattering is a resonant effect, a typical gain bandwidth is ~200 cm⁻¹, leading to overlapping cascade higher order Raman bands. Self-phase modulation broadens these bands even further, leading to a broad-band continuum generation, spectrally shifted to the infrared region. The above described scenario is realized when the incident pulse duration is long enough to avoid significant spectral broadening due to self-phase modulation, which results in a homogeneous spectral broadening, and is short enough to benefit overlapping of higher order Stokes lines. In addition, the fiber dispersion should be low enough to ensure the effective energy exchange between higher order Stokes components.

To experimentally realize the described above scenario, we use UHNA3 (ultra-high numerical aperture silica fiber) from ThorLabs, Inc. (operating wavelength 1300 nm, N. A. = 0.35, mode field diameter 3.2 μm). This high numerical aperture is achieved by using a nearly pure GeO₂ core. We used several fiber lengths from as long as 10-m and as short as 50-cm. We operate our laser at the repetition rate of 15 MHz and launch approximately up to 1.8 W (or ~120 nJ per pulse) into the fiber and observe a broadband continuum output as a function

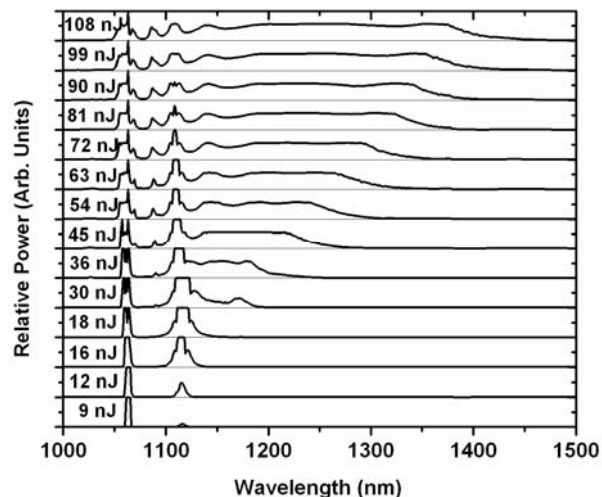


Fig. 2. The development of the spectrum of white-light continuum generated in a 3-m-long GeO₂ fiber as a function of the input energy.

of the incident energy. As much as 40% of the incident power is transmitted through the fiber and is re-collimated with high-numerical aperture aspheric lens (ThorLabs, Inc.). The collimated output of the fiber is then sent to the spectrally and intensity calibrated ½-meter spectrometer with the attached either Si/Ge or liquid-nitrogen-cooled InGaAs detector.

The output spectra are shown in Fig. 2 as a function of the incident pulse energy for the fiber length longer than 3-m. The spectral modulations in the range from 1150 to 1400 nm are much more pronounced for the shorter-length fibers. Fig. 2 clearly represents the described above scenario of spectral formation via stimulated Raman scattering. It is clear from this figure that in order to achieve a smooth spectral broadening from 1150 nm to 1300 nm, corresponding to Raman shifts from 700 to 1700 cm⁻¹), at least 70-nJ of pulse energy is required. At this level of input energy we observe at least 80% of energy conversion into the red-shifted white-light continuum, and more than 60% of the incident energy going into the spectral region from 1150 to 1300 nm. The further increase of the incident energy does not

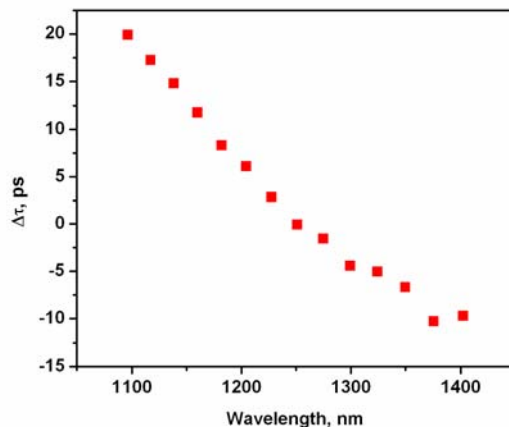


Fig. 3. The relative delay of arrival times of different spectral components of white-light continuum generated in a 3-m-long GeO₂ fiber.

produce a significant increase of the energy of the white light continuum in this particular spectral region, since most of the access energy is transferred into generation of higher Stokes components.

Propagation of short, ultrabroadband laser pulses in a 3-m-long optical fiber results in a substantial temporal broadening of the laser pulse due to the fiber material dispersion. In order to use this continuum for nonlinear Raman spectroscopy, we have to measure the arrival times of different spectral components of the output of the fiber. We used the time-delayed portion of the fundamental for sum-frequency generation (1064 nm + White Light Continuum) in a 1-mm-thick BBO crystal (Type I phase-matching). For each spectral component we find the temporal delay of the fundamental, which produces the best temporal overlap of two pulses, and plot this time-delay (or arrival time of the corresponding spectral component of white light continuum) as a function of the wavelength. This dependence is shown in Fig. 3. Since the original pulse duration is of about 4-ps, it is clear that for any given temporal position of the fundamental, not more than 400 cm^{-1} spectral window is available for nonlinear Raman spectroscopy. To increase this spectral window, we can either move the temporal position of the reference fundamental beam and take spectra for different temporal positions of this pulse, or, alternatively, use a pair of gratings to temporally compress the white-light continuum to match the pulse duration of the fundamental pulse. In our design we used inexpensive Al-coated 600-l/mm gratings (Optometrics, Inc.) and achieved about 10% transmission in double-pass geometry. It still provides us with more than 2 nJ per pulse, which is enough to observe strong nonlinear Raman signals from a tightly focused spot.

4. Experimental results

In order to the performance of our CARS apparatus, we decided to image polystyrene beads in water solution, which were stuck to the surface of a cover slip. These particular beads were $0.5\text{-}\mu\text{m}$ in diameter and were clearly seen in transmission light through an immersion microscope objective (Olympus, Inc., N.A. = 1.30). We used special short-pass mirrors from Omega Optical, Inc. (1050SP or 1100SP) to select the part of the spectrum with wavelength longer than $1.1\text{ }\mu\text{m}$. We find that the set of two mirrors is sufficient to reduce the light intensity of the continuum at the wavelength shorter than $1.0\text{ }\mu\text{m}$ more than 6 orders of magnitude. It gives us enough suppression of the background, which is not related to the actual CARS signal.

However, the major background in any CARS experiment is the so-called “non-resonant” background. It comes from a number of competing pathways of generating signal at the frequency $\omega_{\text{CARS}} = 2\omega_1 - \omega_2$. Most of these pathways do not involve a specific resonant Raman transition and do not carry the valuable information, but the combined intensity of these transitions from a surrounding molecules (typically, water molecules) can be comparable or even greater than a resonantly enhanced nonlinear Raman signal. There are many ways to suppress this non-resonant background [27], such as using polarization spectroscopy, temporal pulse separation [28], and electronic resonance enhancement. Over the last several years most of these techniques were combined with microscopy to get significant (several orders in a contrast ration) discrimination of the useful signal against non-resonant background. Microscopic CARS imaging in a tightly focused, back-reflection geometry (epi-direction) also results in a significant suppression of a non-resonant background [27-28].

We choose the method of polarization CARS, which requires minimal optical elements and is very easy to implement and tune for the best performance [27]. We use a polarization maintaining strain-free microscope objective (Olympus, Inc. ACH100XP (100x, achromat, flat-field, infinity corrected, N. A.=1.25)) and find it satisfactory for our applications.

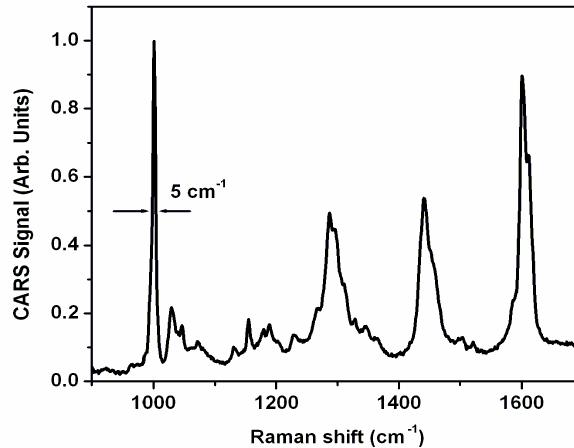


Fig. 4. Broadband resonant CARS spectrum of a single 0.5- μm -diameter polystyrene sphere recorded under microscopic conditions.

The presence of a non-resonant background is, actually, can be very useful for intensity calibration of our spectra. By placing in the focal spot of a microscope objective a material, which does not have any strong Raman lines in the spectral region from 800 to 1700 cm^{-1} , and by removing the polarizer in front of the detector, only a non-resonant contribution to the CARS signal is detected. By recording this non-resonant CARS spectrum, we can store this reference spectrum, which takes into account both the intensity variations of our continuum spectrum and chromatic aberrations of our optical system.

Fig. 4 shows a normalized to the non-resonant background spectrum the resonant CARS spectrum from a single polystyrene bead. The sharpest line of the spectrum has a width (FWHM) of 5 cm^{-1} , providing us with a proof that narrow spectral features can be resolved, while recording a broadband CARS spectrum.

5. Conclusion

Nonlinear Raman microscopy is an emerging technique in cellular biology. We have designed and experimentally tested CARS microscopy system, which cost, including all the laser, delivery, microscopy, and detection systems less than \$50,000. The whole Raman spectrum from 800 to 1700 cm^{-1} can be easily measured with high spectral resolution. We have recently applied this novel spectroscopic system to image collagen structures in tissues [29] and to watch collagen transformation and adhesion in solution [30].

Acknowledgments

The author would like to gratefully acknowledge Prof. R. D. Heathcote (Department of Biology, University of Wisconsin – Milwaukee, USA), Prof. S. Saltiel (Department of Physics, Sofia University, Bulgaria), and Dr. V. Shcheslavskiy (Department of Physics, University of Southampton, UK) for their stimulated discussions and invaluable assistance with experiments. This work is supported by NSF-ECS grant 9984225, NIH grants R21RR14257, R15CA83910 and R21RR14257, Research Corporation Award RI0447, and NATO Collaborative Linkage Grant 979419.